Pulmonary intimal sarcoma: a rare differential diagnosis for arterial filling defects on a chest CT

Lukas Ebner, Adrian Huber, Daniel Ott and Andreas Christe

Abstract

We present a rare case of pulmonary intimal sarcoma mimicking pulmonary embolism in a 40-year-old woman. Although extremely rare, these tumors must be considered in patients who present inappropriate imaging findings that suggest embolism. Chest computed tomography is the modality of choice to determine the extent of the tumor. We present a female patient with suspected embolism that was in fact found to be an endothelial sarcoma of the pulmonary arteries.

Introduction

Intimal sarcoma, especially arising in the lumen of the pulmonary arteries, is an extremely rare and highly malignant tumor of the vessel walls. In general, primary neoplasms of the cardiovascular system are already rare. The prevalence of these tumors ranges from 0.001% to 0.28% within the literature (1). The imaging method of choice is contrast-enhanced chest computed tomography (CT) of the pulmonary arteries, similar to suspected pulmonary embolism. Magnetic resonance imaging (MRI) or positron emission tomography (PET)-CT might also be helpful to detect the enhancement in the luminal mass that indicates a vessel tumor.

We present a rare case of a patient with suspected pulmonary embolism that, in fact, was found to be an intimal sarcoma.

Case report

A 40-year-old woman was admitted to our institution presenting with slowly progressing dyspnea for the last 6 months. She also exhibited non-specific thoracic pain. The discomfort and subjective shortness of breath were initially attributed to musculoskeletal symptoms. Lung function tests demonstrated no significant restriction of the lung volume. A chest CT scan with an intravenous contrast agent was performed to first rule out interstitial lung disease and further pathology of the chest (128 row multislice scanner, Somatom Definition Flash, Siemens Healthcare, Erlangen, Germany; 70 mL of Iomeron 400 i.v. Bracco, Milano, Italy; 4 mL/s flow; reconstructions with 1 and 5 mm axial slice thickness, 5 mm maximum intensity projection in the axial and coronal planes).

Chest CT revealed a left-sided incomplete occlusion of the left main pulmonary artery and peripheral complete occlusions of the segmental braches on the same side. On the right side, the main pulmonary artery was nearly completely occluded by a hypodense structure (Fig. 1a and b). The filling defect started at the level of the pulmonary valve, across the bifurcation of the pulmonary trunk, and showed progression in the central and segmental pulmonary arteries on both sides. In the absence of any obvious enhancement, the obstruction was first interpreted as an embolus. Because of the

Inselspital, University Hospital Bern, Departement for Diagnostic, Pediatric and Interventional Radiology, Bern, Switzerland

Corresponding author:
Lukas Ebner, Inselspital Bern, Universitätsinstitut für Diagnostische, Interventionelle und Pädiatrische Radiologie (DIPR), Departement Radiologie, Neuroradiologie und Nuklearmedizin DRNN, Freiburgstrasse 10, CH-3010 Bern, Switzerland.
Email: Lukas.Ebner@insel.ch

inconsistency of the CT findings and the clinical presentation, concerns arose regarding the potential for another entity, such as a primary tumor of the heart. Next, a high resolution PET-CT scan of the chest was performed (tracer 371 MBq F-18-FDG; Swan Isotopen AG, Bern, Switzerland). The luminal lesions exhibited peripheral FDG uptake, which can indicate tumor tissue but also may be due to granulations in the periphery of a thrombus.

The patient was submitted to surgery. After resection of the pulmonary trunk, the surgeons delivered a myxoid tumor adherent to the pulmonary valve (Fig. 2a and b). Intraoperative histological evaluation revealed an intimal neoplasia arising from the vessel wall (Fig. 2c). During the same procedure, the surgeons removed the affected valve, the pulmonary trunk, and both pulmonary arteries. A valve-bearing conduit connecting the right outflow tract to the distal pulmonary artery on the right was placed. The left lung was then resected. At the 1-year follow-up examination, we found a tumor recurrence along the right cardiophrenic angle and multiple pleural metastases on chest CT (Fig. 3). Despite operative revision, tumor recurrence was evident on a follow-up MRI at 6 months (3 T MRI scanner, Skyra, Siemens Healthcare, Erlangen,
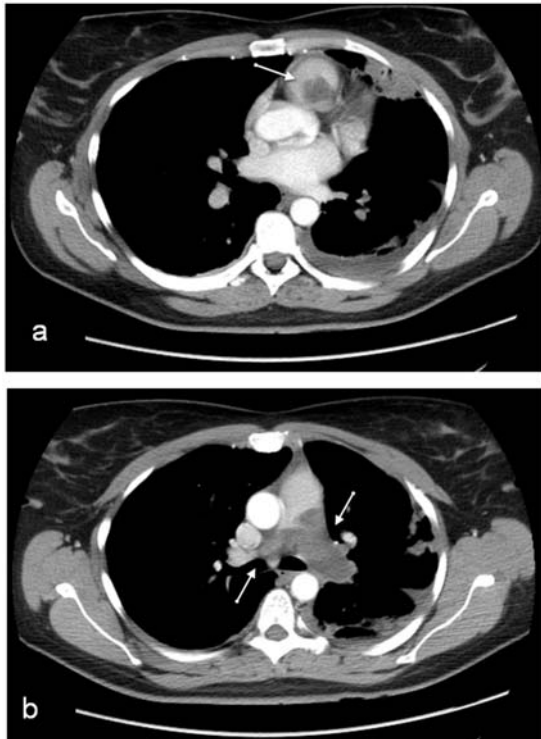
Fig. 1. Axial chest CT with intravenous contrast. (a) Filling defect in the pulmonary trunk (arrow), suggesting central pulmonary embolism. Central filling defects in both pulmonary arteries that extend beyond the bifurcation can be observed (b). There is further consolidation in the lingula segment. Pleural effusion on the left.

Fig. 3. On the follow-up CT scan, the arrow points towards the malignant implantation along the right cardiophrenic angle. There is broad contact with the pericardial sac. The hypodense enhancement pattern indicates myxoid differentiation. Pneumonectomy of the left side.

Fig. 2. Intraoperative presentation corresponding to Fig. 1. (a) Neoplasm adherent to the pulmonary trunk (arrow). The tumor tissue extends just to the level of the pulmonary valve (dashed arrow). View in the right ventricle along the outflow tract. (b) Left lung after pneumonectomy. Complete tumor occlusion of the left main pulmonary artery (circle). The myxoid stroma of the neoplastic tissue can be observed. (c) Slide (HE-staining). The slide represents a cross-section of the pulmonary artery. The myxoid stroma is completely occluding the lumen (asterisk). The arrow points at the vessel wall.
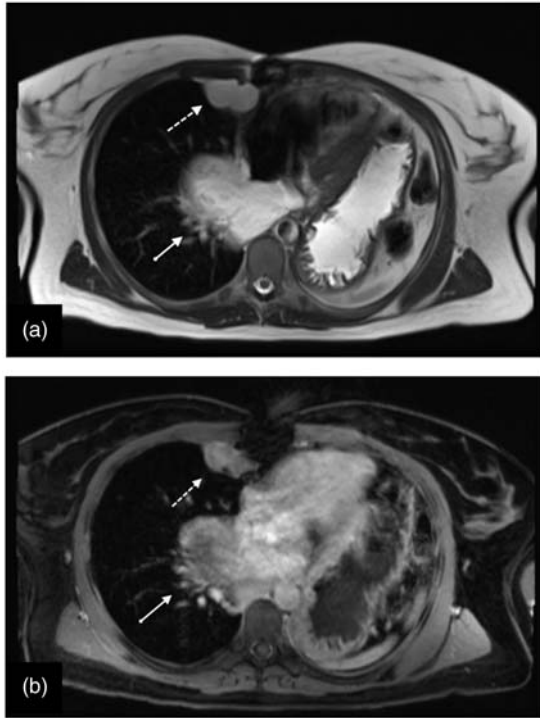
Fig. 4. Follow-up MRI after two-fold revisions. (a) On the axial T2-weighted image (HASTE sequence), a tumor recurrence along the right cardiophrenic angle can be observed (dashed arrow). Additionally, there is a mass-like tumor on the right side adjacent to the pericardium (arrow). On the fat-saturated FLASH sequence, both lesions exhibit marked enhancement (b).

Germany; chest and abdomen; 7.5 mL MultiHance i.v., Bracco Suisse SA; protocol consisted of Haste axial/coronal; Trufi axial; Flash 2 axial fat sat axial; T1 Vibe fat sat coronal; Flash 3D dynamic acquisition coronal) with a recurrence of the involvement of the right cardiophrenic angle. An infradiaphragmatic tumor that had spread through the phrenic hiatus along the inferior caval vein into the liver was observed. Furthermore, there was concern of a new pericardial implantation with continuous invasion of the pericardial sac (Fig. 4a and b). Because of the extent of the local tumor and its inoperability at this stage, palliative care was carried out.

Discussion

Theoretically, neoplasms of the pulmonary arteries can be grouped by their primary location: (i) extraluminal tumors; (ii) intraluminal carcinomas; and (iii) mixed types (2). Histologically, these neoplasms can be divided into angiosarcomas, which arise from the intimal cell layers, and soft tissue sarcomas with mesenchymal descent (myofibroblastic, muscular, or osseous and chondral differentiation). Diagnostic clues to

angiosarcomas include the expression of the factor VIII antigene or evidence of the so-called Weibel-Palade bodies (3). Involvement of the P53 gene in the evolution of angiosarcomas is also discussed. However, angiosarcoma can be induced by exogenous stimulation as former use of Thorotrast (a former contrast agent) and mediastinal radiation for other tumors. The most common locations for sarcomas of the vessel wall include the inferior caval vein, the pulmonary veins, and the heart. However, manifestations in the pulmonary arteries are rare (4). Epidemiologic data indicate that the first diagnosis peaks at the age of 50 years. There is no gender predominance. The clinical symptoms are strongly dependent on the site of tumor manifestation. Occlusion of the pulmonary arteries mimics a pulmonary embolus. Symptoms such as dyspnea, shortness of breath, chest pain, and hemoptysis are often present. Tumor involvement of the superior caval vein may manifest with superior congestion, soft tissue edema, or headache. In contrast, tumor occlusion of the inferior caval vein can spread into the liver parenchyma and manifest as a Budd-Chiari appearance. The mode of dissemination is primarily hematogenous. Metastases are found in the lungs, brain, bones, and pleura (5). Depending on the location, surgical resection is the main therapeutic option. Stenting and conduit placement offer further possibilities for therapy. Imaging is mostly performed using contrast-enhanced CT to visualize the vascular pathology. The most characteristic finding is a vascular filling defect with varying enhancement of the so-called "pseudo-clot". Otherwise, enhancement in a filling defect virtually excludes thrombus. Further CT findings include the following: lobulated filling defects, extension beyond the vessel lumen and metastases (most often to the lung and bones). In some cases, MRI may better depict the enhancement pattern of the neoplasm (6).

The radiographic findings in this case were non-specific; enlargement of the pulmonary arteries or lung nodules can be seen. A recent publication by Attinà et al. investigated the role of PET-CT in the differentiation of chronic pulmonary embolism from pulmonary intimal sarcomas. Based on increases in radiopharmaceutical uptake, PET-CT is able to reliably distinguish between chronic arterial filling defects and tumor tissue. A PET-CT revealing tracer uptake at the level of the arterial filling defect that exceed values of standardized uptake value (SUV) suggest malignancy. In contrast, thrombi generally do not exhibit increased tracer activity. In the case of a chronic embolism, a slight increase in activity may be observed (7).

In conclusion, one should always consider vascular neoplasms when pulmonary filling defects are suspected after observing enhancement within the clot or if the clinical setting is inappropriate.

Vascular filling defects that expand the vessel lumen or grow outside the vessel wall are almost certainly aggressive carcinomas. Invasion of the adjacent structures indicates a local tumor that extends beyond the vessel wall.

References

1. Mader MT, Poulton TB, White RD. Malignant tumors of the heart and great vessels: MR imaging appearence. Radiographics 1997;17:145–153.
2. Kreft B, Flacke S, Zhou H, et al. Diagnostic imaging of vascular leiomyosarcomas. Rofo 2004;176:183–190.
3. Kumar V, Ramzi SC, Stanley LR (eds). Basic Pathology. Saunders, 1997:304–305.
4. Barth J, Lehmann H, Thermann M, et al. Rhabdomyosarcoma of the pulmonary artery. Rofo 1982;136:669–672.
5. Kim JH, Gutierrez FR, Lee EY, et al. Primary leiomyosarcoma of the pulmonary artery: a diagnostic dilemma. Clin Imaging 2003;27:206–211.
6. Yi CA, Lee KS, Choe YH, et al. Computed tomography in pulmonary artery sarcoma: distinguishing features from pulmonary embolic disease. J Comput Assist Tomogr 2004;28:34–39.
7. Attinà D, Niro F, Tchouanté P, et al. Pulmonary artery intimal sarcoma. Problems in the differential diagnosis. Radiol Med 2013;118:1259–1268.